Theriogenology. Author manuscript; available in PMC 2010 October 15.

Published in final edited form as:
Theriogenology. 2009 October 15; 72(7): 902–909. doi:10.1016/j.theriogenology.2009.06.006.

Evaluation of the ultrasound image attributes of developing ovarian follicles in the four follicular waves of the interovulatory interval in ewes

B.M. Toosi[a], **S.V. Seekallu**[a], **R.A. Pierson**[b], and **N.C. Rawlings**[a,*]

[a] Department of Veterinary Biomedical Sciences, Western College of Veterinary Medicine, University of Saskatchewan, Saskatoon, Saskatchewan, S7N 5B4, Canada

[b] Department of Obstetrics, Gynecology and Reproductive Sciences, College of Medicine, University of Saskatchewan, Saskatoon, Saskatchewan, S7N 0W8, Canada

Abstract

Computer-assisted quantitative echotextural analysis was applied to ultrasound images of antral follicles in the follicular waves of an interovulatory interval in sheep. The ewe has three or four waves per cycle. Seven healthy, cyclic Western White Face ewes (*Ovis aris*) underwent daily, transrectal, ovarian ultrasonography for an interovulatory interval. Follicles in the third wave of the ovulatory interval had a longer static phase than that of those in Waves 1 and 2 ($P < 0.05$). The numeric pixel value for the wall of anovulatory follicles emerging in the third wave of the cycle was significantly higher than that for Waves 1 and 2 at the time of emergence (156.7 ± 8.09, 101.6 ± 3.72, and 116.5 ± 13.93, respectively), and it decreased as follicles in Wave 3 reached maximum follicular diameter ($P < 0.05$). The numeric pixel value of the antrum in the ovulatory follicles decreased as follicular diameter increased to ≥5 mm in diameter ($P < 0.05$). The pixel heterogeneity of the follicular antrum in Wave 1 increased from the end of the growth phase to the end of the regression phase for follicles in that wave ($P < 0.05$). The total area for the wall and antrum of the follicles studied were correlated with follicular diameter in all follicular waves ($r = 0.938$, $P < 0.01$ and $r = 0.941$, $P < 0.01$ for the wall and antrum, respectively). Changes in image attributes of the follicular wall and antrum indicate potential morphologic and functional differences among antral follicles emerging at different stages of the interovulatory interval in cyclic ewes.

Keywords

Echotexture; Image analysis; Ovarian follicle; Sheep; Ultrasound

1. Introduction

Ultrasonographic imaging of the reproductive tract is well developed in several domestic animal species [1–7]. Particular emphasis has been placed on enhancing our understanding of ovarian function [4–9]. Imaging allows repeated, noninvasive, visual assessment of

*Corresponding author. Tel.: +1 306 966 7373x1324; fax: +1 306 966 7376. norman.rawlings@usask.ca (N.C. Rawlings).

changes in ovarian structures over time [10]. Using ultrasonography, wave-like patterns of follicular development were reported in sheep [4,6,7]. An antral follicular wave in the ewe is defined as the emergence or growth of one to three follicles from a pool of small follicles (1 to 3 mm in diameter); the follicles attain diameters of ≥5 mm before regression (anovulatory wave) or ovulation (ovulatory wave) [11,12]. The average interwave interval is 4 to 5 d, and 3 or 4 follicular waves emerge in each interovulatory interval [11,12].

Ultrasonography is based on the ability of body tissues to reflect or transmit high-frequency sound waves [9,13]. Reflection or echo of the ultrasound beams depends on the relative density and microstructural organization of the tissue [9,14]. An ultrasound image is a two-dimensional array of picture elements called pixels [15]. Each pixel represents one of 256 shades of gray ranging between 0 (black) and 255 (white) [10,15]. The human eye is capable of distinguishing among only 18 to 20 shades of gray [15]; therefore, quantitative evaluation of the changes in the ultrasonographic appearance of the tissue (echotexture) is not feasible by the human eye [10]. Complex computer algorithms were designed to objectively analyze and quantify the range of 256 shades of gray of pixels in ultrasound image echotexture [9,10].

Identification of the various phases of the life span of follicles (growing, static, and regression phases) is only feasible with retrospective examination of ultrasonographic data collected daily [9,10,16]. The phases of the life span of antral follicles and their physiologic function have been shown to be associated with histomorphologic characteristics of follicles [16–19]. Therefore, image attributes of follicles, representing histomorphology, can be used to assess stage of development and aspects of physiologic function [16,17]. The validity of image analysis to predict the physiologic status of ovarian follicles has been tested in domestic species, mainly cattle, by evaluating correlations among ultrasound image characteristics and histomorphologic and functional attributes of follicles and oocyte viability [16–18,20,21]. Image attributes of antral follicles in cattle were found to be related to the cellular and vascular composition of the follicular wall and to some aspects of secretory activity of the follicle [16]. Image analysis may eventually allow prediction of the viability of an antral follicle and the oocyte it contains [9,10,18].

Our objective was to determine if ultrasonographic image attributes would be indicative of changes during development and regression of antral follicles in follicular waves in the normal cyclic ewe. Because subsequent waves develop at different phases of the cycle and therefore under different endocrine milieus, we hypothesized that ultrasound image attributes of antral follicles would change with the stages of development and regression within a follicular wave and would also differ among the different follicular waves in an estrous cycle.

2. Materials and methods

2.1. Animals

All animal experimentation was performed in compliance with the guidelines of the Canadian Council on Animal Care and was approved by the local animal care committee. Seven healthy, normally cycling, nulliparous Western White Face ewes (*Ovis aris*), 6 to 7 yr

of age (average body weight 79.9 ± 4.12 kg), were used in this study (November to December). All ewes were housed indoors with lighting set to simulate the natural light/dark cycle.

Animals received daily maintenance rations of alfalfa pellets with water, hay, and cobalt iodized salt licks available ad libitum. Estrus was synchronized by application of a progestogen-releasing intravaginal sponge for 14 d (medroxyprogesterone acetate, 60 mg; Veramix; Pharmacia & Upjohn Animal Health, Orangeville, ON, Canada). Estrus was detected with two vasectomized crayon-harnessed rams. The study was conducted in the second cycle after synchronization.

2.2. Ultrasonography

All ewes underwent daily transrectal ovarian ultrasonography with an instrument (Aloka SSD 900; Aloka Co. Ltd., Tokyo, Japan) equipped with a stiffened 7.5-MHz linear-array transducer. Ultrasonographic examination of the ovaries began 2 d before the expected day of estrus and continued for a complete interovulatory interval. The day of ovulation was defined as the day on which an ovarian follicle ≥5 mm in diameter, which had been previously identified, was no longer seen [11]. Images of all ovarian follicles ≥3 mm in diameter were recorded on high-grade video tape (Fuji S-VHS, ST-120 N; Fujifilm, Tokyo, Japan) using a compatible VCR (Panasonic, Super VHS, AG 1970; Matsushita Electronic of Canada Ltd, Mississauga, ON, Canada) for image analysis. All equipment and machine settings (near-field, far-field, and overall gain) were standardized for optimal ovarian imaging and the settings maintained for the study. The diameter and relative position of all follicles ≥3 mm in diameter were also sketched on ovarian charts to identify follicular waves and map the patterns of growth and regression of follicles in the waves. The length of the growth, static, and regression phases for anovulatory follicular waves were calculated as previously defined [11].

2.3. Image acquisition and analysis

Image analysis was performed for one follicle per wave (growing from 3 mm to ≥5 mm in diameter). For consistency, when there was more than one follicle in a wave, the follicle that emerged first was analyzed. Images of follicles collected daily from emergence (3 mm in diameter) to regression (3 mm in diameter) or ovulation, which had the greatest cross-sectional diameter, were digitized at standardized settings. The digitized images (resolution of 640 × 480 pixels and 256 shades of gray) were then analyzed with a series of custom-developed computer algorithms optimized for ultrasonography (SYNERGYNE, version 2.8, Saskatoon, SK, Canada).

2.3.1. Image analysis of follicular wall and antrum—The follicular antrum was outlined at the inner boundary of the follicular wall to evaluate its area. The area encompassing the follicular wall was then outlined, and the area located between the outer and inner boundaries was analyzed. This procedure was performed by a single trained individual for all follicles to minimize subjective deviation. The numerical pixel value (NPV) was calculated. This metric is the mean pixel value (MPV) of the gray-scale values of all the pixels within the outlined area. Pixel heterogeneity (PH) was also calculated; this is

defined as the standard deviation of the values of the selected pixels within an area, from the mean pixel value calculated for that area. Area under the curve (AUC) was defined as the area of the sampled region in standard scale-bar units.

2.4. Blood sampling and hormone assays

Blood samples were collected daily (8 to 10 mL) into Vacutainers (Becton Dickinson, Rutherford, NJ, USA) prior to each ultrasound examination and kept at room temperature for 24 h. Serum was then separated and stored at −20 °C until assayed. Serum concentrations of follicle-stimulating hormone (FSH) [22] and progesterone [23] were determined by established radioimmunoassays. The sensitivity of the assays (defined as the lowest concentration of hormone capable of significantly displacing labeled hormone from the antibody) for FSH and progesterone were 0.1 and 0.03 ng/mL, respectively. For reference sera with mean FSH concentrations of 0.93 or 3.76 ng/mL, the intra-assay and interassay CVs were 6.1% or 3.4% and 6.1% or 3.2%, respectively. The intra-assay and interassay CVs were 13.2% or 6.3% and 12.1% or 5.9%, respectively, for reference sera with mean progesterone concentrations of 0.26 or 1.06 ng/mL. Peaks in serum concentrations of FSH, in samples taken daily, were detected using a cycle detection computer program [24].

2.5. Statistical analysis

Follicular wave characteristics (Table 1) were compared among different waves by one-way repeated measures ANOVA (SigmaStat Statistical Software for Windows, version 2.03; SPSS Inc., Chicago, IL, USA). To investigate daily changes of image attributes over the follicular life span within each wave and compare these attributes among different waves, data were normalized to the first day of follicular life span and analyzed by two-way repeated measures ANOVA (SigmaStat Statistical Software for Windows, version 2.03; SPSS Inc.). Main effects were day in follicular life span and wave in the interovulatory interval, with day by wave interaction. Multiple comparisons were made by Fisher's least significant difference (LSD). Correlations between follicular diameter and the area under the curve for the follicular wall and antrum, as well as correlations among the serum progesterone concentrations and image attributes of the follicular wall and antrum were analyzed using Pearson's correlation (SigmaStat Statistical Software for Windows, version 2.03; SPSS Inc.). All values are means ± SEM.

3. Results

3.1. General results

The mean length of the interovulatory interval was 18.3 ± 0.32 d. In six ewes, four distinct follicular waves were detected during the ovulatory interval, whereas one ewe had three waves. Emergence of each follicular wave was associated with a transient peak in circulating FSH concentrations (Fig. 1). Follicular Waves 1 and 3 in the ewe with three waves emerged on Days 1 and 12 of the interovulatory interval, respectively. These days were the same as the days of emergence for Waves 1 and 4 in the rest of the animals; therefore, data were pooled for analysis. In the ewe with three waves, Wave 2 emerged ~2 d later (Day 6) than Wave 2 in the rest of the ewes and therefore was excluded from analysis. There was no difference in the length of the growth (2.7 ± 0.25 d) and regression (2.8 ± 0.23 d) phases

between different waves ($P > 0.05$; Table 1; Fig. 1). The mean length of the static phase was greater in Wave 2 ($P < 0.05$) compared with that of other waves (Table 1; Fig. 1).

3.2. Numerical pixel value of the follicular wall and antrum

No changes were observed in the NPV of the follicular wall in the first and second waves of the ovulatory interval as the follicles grew from 3 to ≥5 mm and then regressed to 3 mm in diameter ($P > 0.05$; Fig. 2). The mean NPV for the wall of anovulatory follicles, emerging in the third wave of the interovulatory interval, was higher than for Waves 1 and 2 at the time of emergence ($P < 0.01$; Fig. 2). For Wave 3, the mean NPV for the wall decreased to a minimum as the follicles reached their maximum follicular diameter ~3 d after emergence ($P < 0.05$). The NPV of the wall for follicles in the ovulatory wave (last wave of the interovulatory interval) tended to decrease as they gained maximum follicular diameter ($P = 0.07$). The mean NPV for the follicular antrum in the first, second, and third waves of the interovulatory interval did not change as the follicular diameter increased from 3 to ≥5 mm and then decreased to 3 mm by the end of regression ($P > 0.05$; Fig. 2). The mean NPV of the antrum for the ovulatory follicles decreased, whereas the follicular diameter increased from 3 mm to its maximum diameter ($P < 0.05$).

3.3. Pixel heterogeneity of the follicular wall and antrum

The pixel heterogeneity (PH) of the follicular wall did not change with growth and regression of follicles in each follicular wave and did not differ among different waves in the interovulatory interval ($P > 0.05$; Fig. 3). Pixel heterogeneity for the follicular antrum in the first follicular wave of the interovulatory interval increased between the end of the growth phase and the late regression phase of follicular development ($P < 0.05$); however, no significant pattern was observed for changes in pixel heterogeneity for the follicular antrum in other follicular waves (Fig. 3).

3.4. Area under the curve for the follicular wall and antrum

The area under the curve for both the follicular wall and antrum were correlated with follicular diameter in all follicular waves ($r = 0.938$, $P < 0.01$ and $r = 0.941$, $P < 0.01$ for the wall and antrum, respectively). The mean area under the curve for the follicular wall and antrum increased in all waves as follicular diameter increased and then decreased in anovulatory waves while follicles regressed ($P < 0.01$; Fig. 4).

3.5. Serum progesterone concentrations

Mean serum progesterone concentrations increased gradually between Days 2 and 11 after ovulation as the corpora lutea formed. Mean serum progesterone concentrations reached a peak of 2.2 ± 0.45 ng/mL on Day 12 after ovulation ($P < 0.01$). Luteolysis resulted in a dramatic drop in serum progesterone concentrations to basal levels on Day 16 after ovulation ($P < 0.01$). Serum progesterone concentrations were not correlated with changes in the numeric pixel value and pixel heterogeneity of the follicular wall and antrum in any follicular wave ($P > 0.05$).

4. Discussion

Our hypothesis that ultrasound image attributes of antral follicles reflect the phases of follicle development and regression over an interovulatory interval was partially supported. We observed a wave-dependent alteration in the image attributes of antral follicles. The mean pixel value of the follicular wall in Wave 3 was higher than that of previous anovulatory waves of the ovulatory interval (Waves 1 and 2) at the time of emergence, and the wall of the follicles in Wave 3 became darker (decreased NPV) as follicular diameter increased. A similar tendency was also seen for ovulatory follicles (Wave 4; $P = 0.07$). No trend in NPV was seen for Waves 1 and 2. Echotexture of the follicular wall is dependent on the thickness of the wall, degree of vascularization in the theca layer, vascular blood flow, and the amount of lipid in steroid-producing granulosa and theca cells [16,17,19,25]. Investigations in cattle revealed that hypertrophy and proliferation of granulosa and theca cells, as well as development of the dense connective tissue of vascular walls, were reflected as brighter images with increased NPV [16,17,26]. However, increased blood flow alters the proportion of vascular tissue to blood and results in a lower NPV in the follicular wall [17]. These changes may reflect alterations in the biological function of follicles [16,17,26,27]. The reason(s) for the higher NPV of the follicular wall in Wave 3 at emergence, as observed in this study, was not clear and requires histomorphologic investigation.

The decreasing NPV of the wall in follicles emerging after the mid-interovulatory interval may be related to increased blood flow, as growing follicles develop to become mature ovulatory sized structures. Tom et. al. [20] reported a rapid decrease in NPV of the follicular wall during the growth of ovulatory follicles and during the transition into the static phase of dominant anovulatory follicles in cattle. Histologic evaluation in the same study revealed high vascularity in the follicular wall. In another investigation in cattle, the wall of preovulatory follicles had low granulosa cell density and high vascularity and edema within the theca interna [19]. Preovulatory follicles destined to develop functional corpora lutea in cattle and humans had a lower NPV (darker) for the follicular wall than that of atretic follicles [16,17,28]. It has been suggested that echotextural characteristics of the follicular wall are indicative of the steroidogenic activity of the theca and granulosa cells in cattle [16]. In ewes given equine chorionic gonadotropin (eCG), high NPV for the follicular wall was associated with higher serum progesterone concentrations after ovulation and CL (corpus luteum) formation [25]. Based on the current echotextural analysis of the follicular wall in cyclic ewes, we speculated that follicles emerging after the middle of the interovulatory interval may be more adapted for ovulation and CL formation. In normal cyclic ewes, ovulation normally occurs from the last wave of the cycle; however, in some prolific breeds of ewes, follicles from the penultimate wave of the cycle can ovulate [11]. Short-term treatment with medroxyprogesterone acetate (MAP) releasing intravaginal sponges at midcycle, after induction of luteolysis with $PGF_{2\alpha}$, can induce follicles from both waves to ovulate in Western White Face sheep [25,29]. It is exciting to note that the NPV of the walls of follicles emerging after the middle of the interovulatory interval differed from that of the walls of follicles of Waves 1 and 2 of the ovulatory cycle. The reasons for this contrast could be investigated further by parallel histomorphologic and functional evaluation of follicles at different time points of the interovulatory interval.

Granulosa cells are sloughed into the antrum individually or as clusters of cells during the later stages of follicular development [16,19]. This may cause an increase in the NPV of the antrum, especially near the follicular wall. In the current study, echotextural analysis of the whole follicular antrum did not reveal significant changes in pixel values in Waves 1, 2, and 3 of the interovulatory interval. This observation was in agreement with results of another report that the mean pixel values of the antrum in bovine anovulatory dominant follicles did not vary significantly during the follicular life span [17]. However, other studies in cattle had brighter (higher NPV) follicular antra during the late-static and regression phases of anovulatory follicles [18]. In the current study, there was a decrease in the NPV of the follicular antrum in ovulatory follicles as they reached their maximum diameter. A tendency for a similar drop in the NPV as the diameter of the follicular antrum increased was also noted for Waves 2 and 3 of the interovulatory interval ($P = 0.09$ and $P = 0.07$, respectively; Fig. 2). This trend might be related to the growth of follicles and the increase in antral fluid volume with low echodensity. The drop in NPV occurred as follicles attained their maximum steroidogenic potential. For ovulatory follicles, the more obvious drop in NPV of the follicular antrum as the follicles grew may represent less cellular debris in the antrum compared with earlier waves in the interovulatory interval. In the ewe, the formation of short-lived CL after multiple gonadotropin-releasing hormone (GnRH) administrations was related to a greater NPV of the central antrum prior to GnRH treatment [27]. This was interpreted to suggest that follicles forming into optimal luteal structures shed greater numbers of granulosa cells into their antra in comparison with follicles forming normal corpora lutea [27].

A significant alteration in PH of the follicular antrum occurred only in the first wave of the interovulatory interval in the current study. The increase in PH of the follicular antrum in Wave 1 of the interovulatory interval started from the beginning of the static phase and continued through the regression phase of the follicular life span (Fig. 3). This could be explained by the accumulation of echoic cellular debris and macromolecules within the follicular antrum [9,16,17]; however, this pattern was not observed in the other anovulatory waves of the interovulatory interval. The follicular wall in preovulatory bovine follicles had low values for PH [16]; however, in the current study, the PH of the follicular wall in the ovulatory wave did not change as the follicles grew to ovulatory diameters. Ovarian antral follicles are much smaller in the ewe than in cattle or humans, and this may account for the high variation in the gray-scale pixel values that we observed. Using regional echotextural analysis requires selection of the whole area of the follicular wall and/or antrum for analysis [9,30]. Because of irregularities at the follicular wall–antrum interface and the small size of ovine ovarian follicles, it is inevitable that some pixels from each region (wall or antrum) enter into the analysis of the other region, resulting in greater variation or heterogeneity in pixel values.

In the current study, the length of the static phase was longer for the follicles emerging in the second wave of the interovulatory interval. Studying the same breed of ewes, Bartlewski et al. [11] reported an extended static phase for the follicles emerging in Wave 1 and a longer growing phase for the follicles in Wave 4 of an interovulatory interval, whereas other wave dynamics remained unchanged. These results lead us to conclude that the pattern of growth and regression of follicles do not vary consistently among the waves of the estrous cycle in

the ewe. This is interesting, as the first and last waves would develop against a background of increasing and decreasing serum progesterone concentration, respectively, whereas Waves 2 and 3 develop largely in an environment of high serum progesterone concentration.

Quantitative assessment of the area under the curve (AUC), combined with follicular diameter data, may assist in interpretation of echotextural data, especially for the follicular wall. An increase or decrease in follicular diameter with no change in AUC for the follicular wall suggests a decrease or increase in the thickness of follicular wall, respectively. Variation in the AUC for both follicular wall and antrum were highly correlated with changes in the follicular diameter. Perhaps changes in the image attributes of the follicular wall were mainly due to alterations in follicular size rather than the wall thickness. However, this assumption must be verified by measurements of follicular wall thickness using histologic sections or computer-assisted programs.

In summary, results from this study partially supported the hypothesis that follicular image attributes change during the life span of follicles within a follicular wave, reflecting the developmental stage of the follicle. Interestingly, the changes were dependent on the time of wave emergence during the interovulatory interval. A greater alteration in NPV of the follicular wall was observed in follicular waves emerging after the middle of the interovulatory interval, suggesting morphologic changes in the wall related to the potential for ovulation of those follicles. The NPV of the antrum in the fourth wave of the interovulatory interval also decreased as these ovulatory follicles grew to ≥5 mm in diameter. This might be indicative of less atretic granulosa cells and other debris in the follicular antrum, suggesting a different morphologic and functional status of follicles destined for ovulation and formation of corpora lutea. Pixel heterogeneity of the antrum in the first wave of the interovulatory interval increased during the static and regression phases of the follicular life span. There were potential morphologic and functional differences among antral follicles emerging at different stages of the interovulatory interval in cyclic ewes. These findings also suggested the predictive potential for image analysis as a diagnostic tool to evaluate follicular physiologic status in sheep.

Acknowledgments

The authors thank Mr. J. Deptuch for his technical assistance with computer-assisted image analysis and Ms. S. Cook and Ms. K. Tran for their help in RIA. The current study was funded by a National Science and Engineering Research Council grant to NCR. Image analysis was performed in the Women's Health Imaging Research Laboratory at the University of Saskatchewan. Both B.M.T. and S.V.S. were recipients of University of Saskatchewan Graduate Student Scholarships.

References

1. Pierson RA, Ginther OJ. Ovarian follicular populations during early pregnancy in heifers. Theriogenology. 1986; 26:649–59. [PubMed: 16726232]
2. Adams GP, Griffin PG, Ginther OJ. In situ morphologic dynamics of ovaries, uterus, and cervix in llamas. Biol Reprod. 1989; 41:551–8. [PubMed: 2686763]
3. Kulick LJ, Kot K, Wiltbank MC, Ginther OJ. Follicular and hormonal dynamics during the first follicular wave in heifers. Theriogenology. 1999; 52:913–21. [PubMed: 10735130]
4. Ravindra JP, Rawlings NC, Evans AC, Adams GP. Ultrasonographic study of ovarian follicular dynamics in ewes during the oestrous cycle. J Reprod Fertil. 1994; 101:501–9. [PubMed: 7932387]

5. Schrick FN, Surface RA, Pritchard JY, Dailey RA, Townsend EC, Inskeep EK. Ovarian structures during the estrous cycle and early pregnancy in ewes. Biol Reprod. 1993; 49:1133–40. [PubMed: 8286581]

6. Souza CJ, Campbell BK, Baird DT. Follicular dynamics and ovarian steroid secretion in sheep during the follicular and early luteal phases of the estrous cycle. Biol Reprod. 1997; 56:483–8. [PubMed: 9116150]

7. Ginther OJ, Kot K, Wiltbank MC. Associations between emergence of follicular waves and fluctuations in FSH concentrations during the estrous cycle in ewes. Theriogenology. 1995; 43:689–703. [PubMed: 16727660]

8. Bartlewski PM, Vanderpol J, Beard AP, Cook SJ, Rawlings NC. Ovarian antral follicular dynamics and their associations with peripheral concentrations of gonadotropins and ovarian steroids in anoestrous Finnish Landrace ewes. Anim Reprod Sci. 2000; 58:273–91. [PubMed: 10708901]

9. Pierson RA, Adams GP. Computer-assissted image analysis, diagnostic ultrasonography and ovulation induction:strange bedfellows. Theriogenology. 1995; 43:105–12.

10. Singh J, Adams GP, Pierson RA. Promise of new imaging technologies for assessing ovarian function. Anim Reprod Sci. 2003; 78:371–99. [PubMed: 12818654]

11. Bartlewski PM, Beard AP, Cook SJ, Chandolia RK, Honaramooz A, Rawlings NC. Ovarian antral follicular dynamics and their relationships with endocrine variables throughout the oestrous cycle in breeds of sheep differing in prolificacy. J Reprod Fertil. 1999; 115:111–24. [PubMed: 10341729]

12. Duggavathi R, Bartlewski PM, Barrett DM, Rawlings NC. Use of high-resolution transrectal ultrasonography to assess changes in numbers of small ovarian antral follicles and their relationships to the emergence of follicular waves in cyclic ewes. Theriogenology. 2003; 60:495–510. [PubMed: 12763163]

13. Aldrich JE. Basic physics of ultrasound imaging. Crit Care Med. 2007; 35:131–7.

14. Staren ED. Physics and principles of breast ultrasound. Am Surg. 1996; 62:103–7. [PubMed: 8554185]

15. Baxes, GA. Digital Image Processing: Principles and Applications. Wiley; 1994. Fundamentals of digital image processing; p. 13-36.

16. Singh J, Pierson RA, Adams GP. Ultrasound image attributes of bovine ovarian follicles and endocrine and functional correlates. J Reprod Fertil. 1998; 112:19–29. [PubMed: 9538326]

17. Tom JW, Pierson RA, Adams GP. Quantitative echotexture analysis of bovine ovarian follicles. Theriogenology. 1998; 50:339–46. [PubMed: 10732129]

18. Vassena R, Adams GP, Mapletoft RJ, Pierson RA, Singh J. Ultrasound image characteristics of ovarian follicles in relation to oocyte competence and follicular status in cattle. Anim Reprod Sci. 2003; 76:25–41. [PubMed: 12559718]

19. Singh J, Adams GP. Histomorphometry of dominant and subordinate bovine ovarian follicles. Anat Rec. 2000; 258:58–70. [PubMed: 10603449]

20. Tom JW, Pierson RA, Adams GP. Quantitative echotexture analysis of bovine corpora lutea. Theriogenology. 1998; 49:1345–52. [PubMed: 10732071]

21. Duggavathi R, Bartlewski PM, Pierson RA, Rawlings NC. Luteogenesis in cyclic ewes: echotextural, histological, and functional correlates. Biol Reprod. 2003; 69:634–9. [PubMed: 12724274]

22. Currie WD, Rawlings NC. Fluctuation in responsiveness of LH and lack of responsiveness of FSH to prolonged infusion of morphine and naloxone in the ewe. J Reprod Fertil. 1989; 86:359–66. [PubMed: 2502622]

23. Rawlings NC, Jeffcoate IA, Rieger DL. The influence of estra-diol-17beta and progesterone on peripheral serum concentrations of luteinizing hormone and follicle stimulating hormone in the ovariectomized ewe. Theriogenology. 1984; 22:473–88. [PubMed: 16725980]

24. Clifton DK, Steiner RA. Cycle detection: a technique for estimating the frequency and amplitude of episodic fluctuations in blood hormone and substrate concentrations. Endocrinology. 1983; 112:1057–64. [PubMed: 6822203]

25. Liu X, Dai Q, Hart EJ, Barrett DM, Rawlings NC, Pierson RA, Bartlewski PM. Ultrasonographic characteristics of ovulatory follicles and associated endocrine changes in cyclic ewes treated with

medroxyprogesterone acetate (MAP)-releasing intravaginal sponges and equine chorionic gonadotropin (eCG). Reprod Domest Anim. 2007; 42:393–401. [PubMed: 17635777]

26. Liu X, Hart EJ, Petrik JJ, Nykamp SG, Bartlewski PM. Relationships between ultrasonographic image attributes, histomorphology and proliferating cell nuclear antigen expression of bovine antral follicles and corpora lutea ex situ. Reprod Domest Anim. 2008; 43:27–34. [PubMed: 18199255]
27. Liu X, Hart EJ, Dai Q, Rawlings NC, Pierson RA, Bartlewski PM. Ultrasonographic image attributes of non-ovulatory follicles and follicles with different luteal outcomes in gonadotropin-releasing hormone (GnRH)-treated anestrous ewes. Theriogenology. 2007; 67:957–69. [PubMed: 17178147]
28. Martinuk SD, Chizen DR, Pierson RA. Ultrasonographic morphology of the human preovulatory follicle wall prior to ovulation. Clin Anat. 1992; 5:1–14.
29. Bartlewski PM, Duggavathi R, Aravindakshan J, Barrett DM, Cook SJ, Rawlings NC. Effects of a 6-day treatment with medroxyprogesterone acetate after prostaglandin F2 alpha-induced luteolysis at midcycle on antral follicular development and ovulation rate in nonprolific Western white-faced ewes. Biol Reprod. 2003; 68:1403–12. [PubMed: 12606440]
30. Birtch RL, Baerwald AR, Olatunbosun OA, Pierson RA. Ultrasound image attributes of human ovarian dominant follicles during natural and oral contraceptive cycles. Reprod Biol Endocrinol. 2005; 3:12. [PubMed: 15829004]

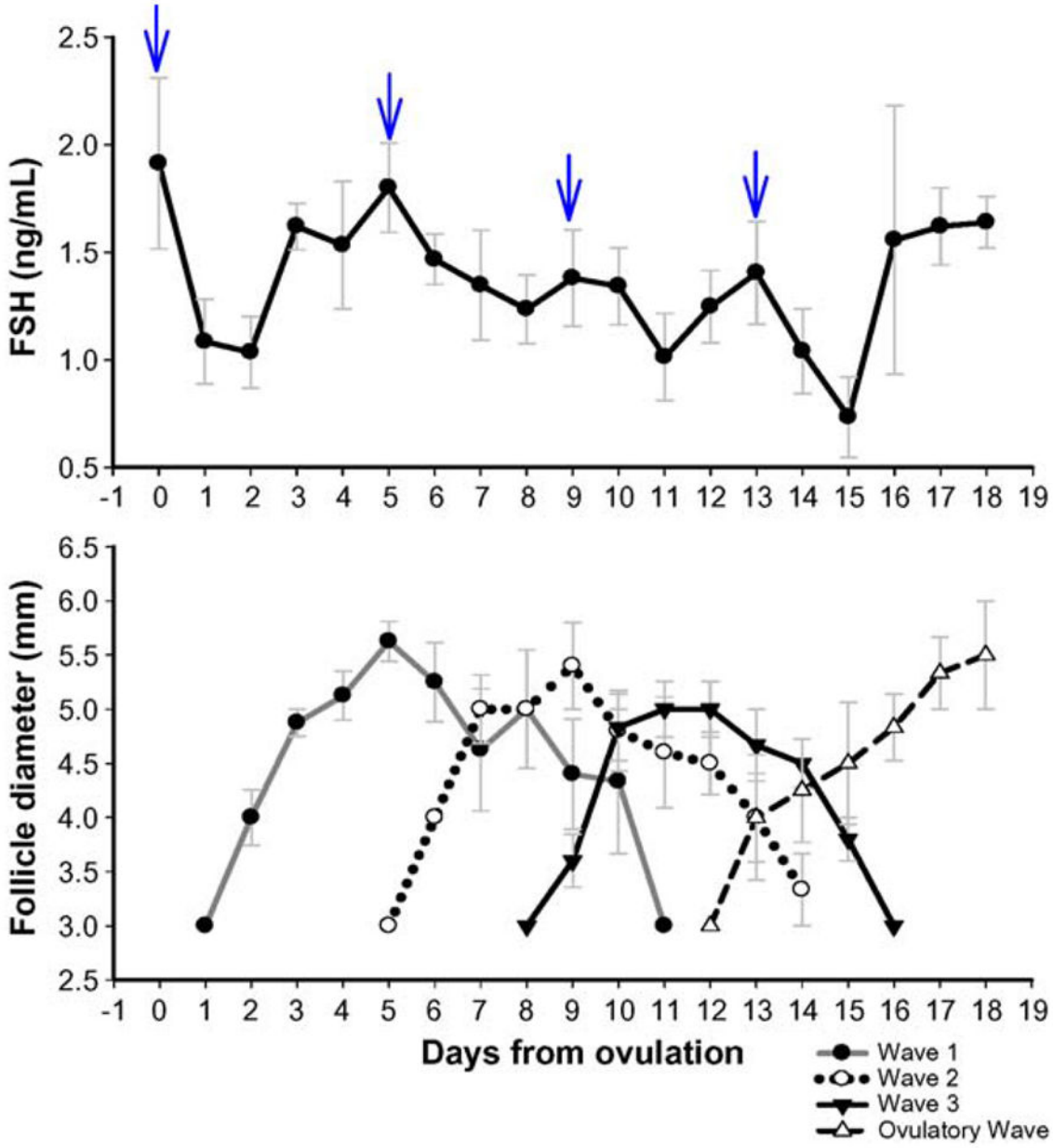

Fig. 1.

Top panel: Mean (±SEM) serum FSH concentrations in cyclic Western White Face ewes. Daily serum concentrations of FSH were normalized to the day of ovulation (Day 0). Arrows indicate peaks in serum concentrations of FSH detected by the cycle detection computer program. Bottom panel: Mean (±SEM) follicular diameter of follicles emerging in different follicular waves during the interovulatory interval in normal cyclic ewes. Data are normalized to the corresponding mean day of wave emergence for each follicular wave after ovulation (Day 0).

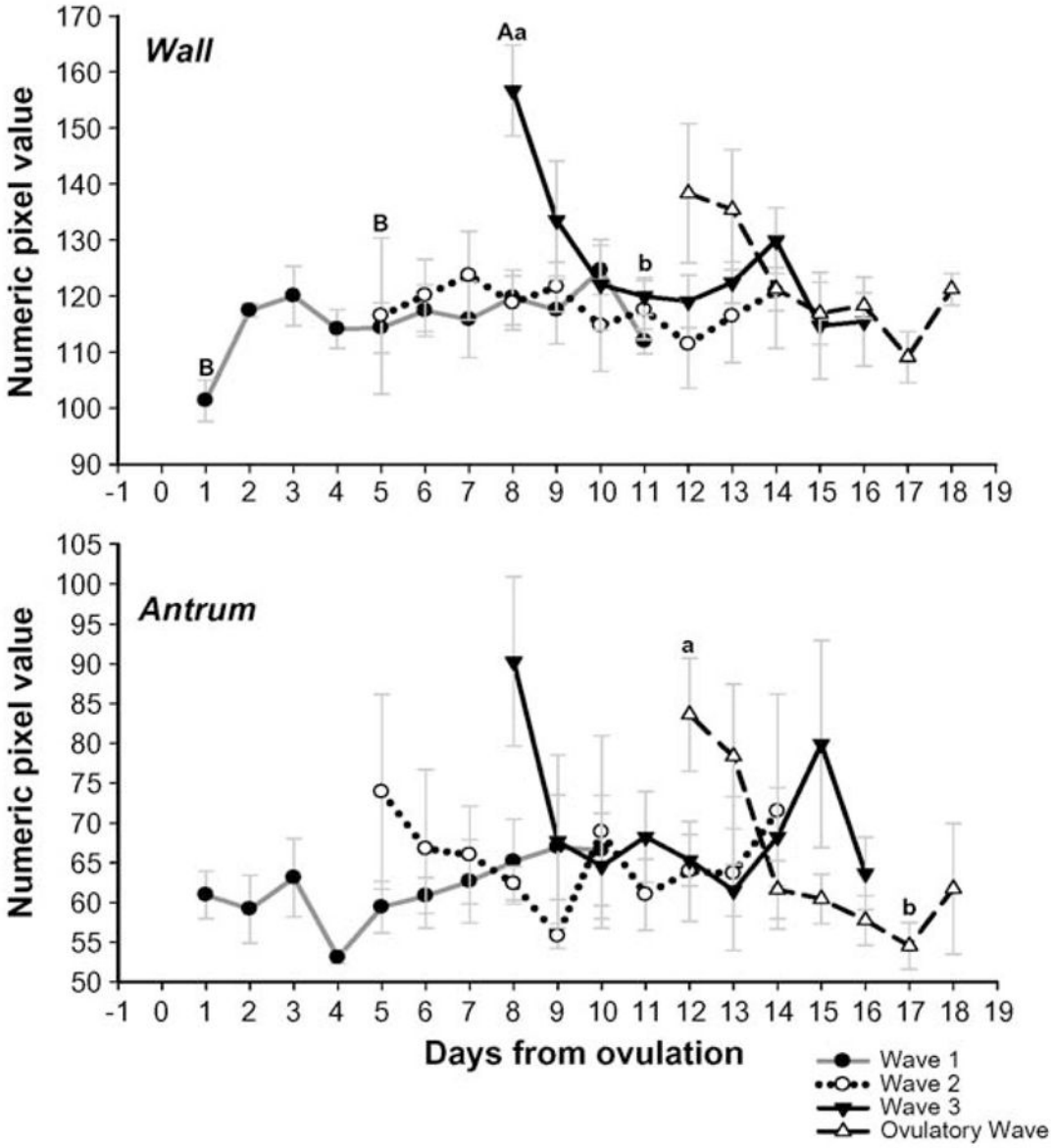

Fig. 2.

Changes in the mean (±SEM) numerical pixel value (NPV) of the follicular wall and antrum (top and bottom panels, respectively) for follicular waves during the interovulatory interval in normal cyclic ewes. Data are normalized to the corresponding mean day of wave emergence for each follicular wave after ovulation (Day 0). [ab]Difference ($P < 0.05$) within days of follicular life span. [AB]Difference ($P < 0.05$) at the time of emergence among different waves.

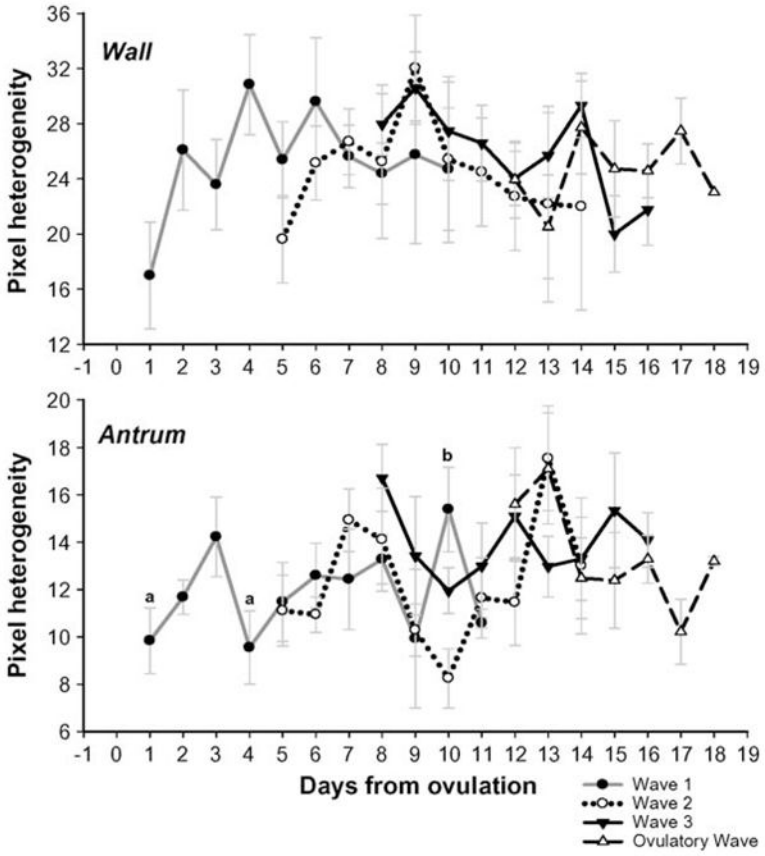

Fig. 3.

Changes in the mean (±SEM) pixel heterogeneity (PH) for the follicular wall and antrum (top and bottom panels, respectively) for follicular waves during the interovulatory interval in normal cyclic ewes. Data are normalized to the corresponding mean day of wave emergence for each follicular wave after ovulation (Day 0). [ab]Difference ($P < 0.05$) within days of follicular life span.

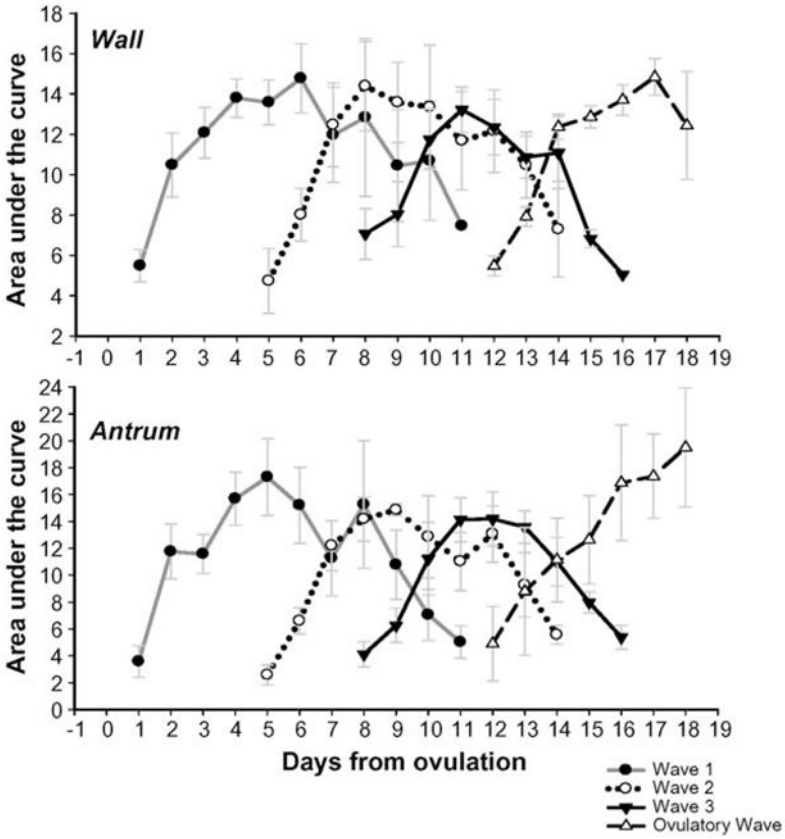

Fig. 4.

Changes in the mean (±SEM) area under the curve (AUC) for the follicular wall and antrum (top and bottom panels, respectively) for follicular waves during the interovulatory interval in normal cyclic ewes. Data are normalized to the corresponding mean day of wave emergence for each follicular wave after ovulation (Day 0).

Table 1

Comparison of wave characteristics (mean ± SEM) for the follicular waves seen during the interovulatory interval in the seven normal cyclic ewes used in this study.

	Follicular waves			
	Wave 1	**Wave 2**	**Wave 3**	**Ovulatory wave**
Number of follicles included in analysis	7	6	7	7
Number of follicles in the wave	1.3 ± 0.23	1.1 ± 0.11	1.2 ± 0.22	1.1 ± 0.09
Day of emergence after ovulation (Day 0)	0.6 ± 0.49^{a}	4.5 ± 0.22^{b}	8.1 ± 0.22^{c}	11.6 ± 0.24^{d}
Growth phase (d)	2.9 ± 0.48	2.5 ± 0.31	2.7 ± 0.57	3.9 ± 0.52
Static phase (d)	1.9 ± 0.33^{a}	3.0 ± 0.42^{b}	1.9 ± 0.63^{a}	1.6 ± 0.38^{a}
Regression phase (d)	2.9 ± 0.48	2.7 ± 0.61	2.7 ± 0.22	—
Growth rate (mm/d)	1.0 ± 0.12	0.9 ± 0.11	1.1 ± 0.19	0.9 ± 0.12
Regression rate (mm/d)	1.0 ± 0.22	1.0 ± 0.21	0.9 ± 0.13	—
Maximum follicular diameter (mm)	5.8 ± 0.25	5.2 ± 0.17	5.3 ± 0.18	5.7 ± 0.33
Interwave interval (d)	W1 to W2: 3.9 ± 0.12	W2 to W3: 3.6 ± 0.24	W3 to W4: 3.5 ± 0.33	

$^{a–d}P < 0.05$.